Graphene-Ink Laminate Structures on Polyvinylidene Difluoride (PVDF) for Pyroelectric Thermal Energy Harvesting and Waste Heat Recovery

Daniel Zabek* [a], Kris Seunarine[b], Chris Spacie[b], and Chris Bowen[a]

[a]University of Bath, Claverton Down, BA2 7AY, Bath, UK.

[b]Haydale Ltd., Ammanford, SA18 3BL, UK.

*email: D.Zabek@bath.ac.uk

Abstract: Thermal energy can be effectively converted into electricity using pyroelectrics, which act as small scale power generator and energy harvesters providing nW to mW of electrical power. In this paper, a novel pyroelectric harvester based on free standing polyvinilidene difluoride (PVDF) was manufactured that exploits the high thermal radiation absorbance of a screen printed graphene-ink electrode structure to facilitate the conversion of the available thermal radiation energy into electrical energy. The use of interconnected graphene nanoplatelets (GNPs) as an electrode enable high thermal radiation absorbance and high electrical conductivity along with the ease of deposition using a screen print technique. For the asymmetric structure, the pyroelectric open-circuit voltage and closed-circuit current were measured, and the harvested electrical energy was stored in an external capacitor. For the graphene-ink/PVDF/aluminium system the closed circuit pyroelectric current improves by 7.5 times, the open circuit voltage improves by 4 times and the harvested energy by 25 times compared to a standard aluminium/PVDF/aluminium system electrode design, with a peak energy density of 1.13 μJ/cm^3. For the pyroelectric device employed in this work, a complete manufacturing process and device characterisation of these structures is reported along with the thermal conductivity of the graphene-ink. The material combination presented here provides a new approach for delivering smart materials and structures, wireless technologies and internet of things (IoT) devices.

Keywords: graphene, ink, PVDF, pyroelectric, piezoelectric, energy harvesting

1. Introduction

Pyroelectric materials have the ability to convert thermal fluctuations into electrical energy, acting as a small scale power supply or thermal energy harvester when connected across an electric load. Harvesting unexplored and untapped thermal energy sources, such as industrial, solar, and geothermal-waste heat or abundantly available heat from friction and the human body, provides an opportunity for local powering of electronic devices, extending battery lifetime, and even allows an accumulated base load power supply for the recovery of otherwise unused, or wasted, thermal energy. In this field, pyroelectric materials enable direct thermal to electrical energy conversion and additionally mechanical to electrical energy conversion via the piezoelectric effect, since all pyroelectrics are also piezoelectric[1]. Based on the change in polarisation dipole moment P_s, the

attracted or repelled surface bound charge is collected at the device electrodes. The sandwich electrode-pyroelectric-electrode structure is then connected to an external electrical load to discharge the generated potential difference as an electrical current. Unlike thermoelectric modules that utilise a spatial temperature difference, pyroelectric energy harvesters require continuous temperature fluctuations induced by an external heat source in order to develop an alternating electrical current[2]. When converting thermal radiation energy, the induced change in temperature is then determined by the radiation absorption coefficient (α) of the exposed electrode material[3]. Popular electrode materials include evaporated or sputtered aluminium films[4], palladium, gold[5] or indium tin oxide (ITO)[6] of metallic nature. These metals have a high thermal conductivity (*k)*, enabling an efficient transfer of heat at the interface between the electrode and the pyroelectric active material, however a low radiation absorption reflects the majority of the available thermal radiation energy. Optimisation approaches aim to reduce reflections and improve thermal conductivity for enhanced heat transfer and energy conversion using pyroelectrics.

From a pyroelectric device perspective, ferroelectric polyvinylidene difluoride (PVDF) is a fascinating material for harvesting thermal and mechanical energy. Compared to ceramic pyroelectric materials, the electrical properties of the ferroelectric β-phase PVDF and the mechanical flexibility, high strain, transparency and good bio-compatibility enables a wide range of applications such as wearable devices[7], wireless sensor nodes, internet of things (IoT) devices, or battery-less technologies. Recently, carbon nano-tube (CNT) modified flexible PVDF harvesters[8], carbon-black composites[9], or micro-patterned electrode structures, have significantly improved the efficiency of pyroelectric energy harvesting devices and their effectiveness[4]. Additional energy conversion improvements are based on the optimisation of the electrode-pyroelectric material architecture. The required transient change in temperature of the device will lead to a thermo-mechanical expansion and contraction, leading to the accumulation of both pyroelectric and piezoelectric activity at the layer interface[10]. According to Newnhman et *al.*, a 2-2 laminate connectivity shows significant improvements of pyroelectric activity when using two dissimilar materials[11]. For conductive heating, mathematical models for various electrode-PVDF-electrode laminates, such as steel, polytetrafluorethylene (PTFE), chlorinated polyvinylchloride (CPVC), aluminium, zinc and Invar 36, show a high piezoelectric activity when combined with a pyroelectric structure. As the electrode thickness decreases, the mechanical strain due to a thermal expansion mismatch improves the pyroelectric coefficient by up to 100 % under open and closed circuit conditions[12]. Despite the thin nature of the metallic electrodes, compared to the pyroelectric active material, it is thought that the shear stress that is developed between the laminate layers significantly contribute to the thermal energy conversion[13]. In contrast, it is reported in the literature that the pyroelectric response with proportionally thick laminates gradually improves to an optimum for equally thick pyroelectric and non-pyroelectric layers[14]. In this paper, asymmetric screen-printed thick film black graphene-ink electrodes on PVDF are studied for pyroelectric harvesting. Due to the high radiation absorption of

the graphene-ink and the thick layered architecture, faster and larger changes in temperature are realised improving pyroelectric device performance. In addition, the free standing irradiated device exhibits mechanical motion during thermal cycling providing both simultaneous pyroelectric and piezoelectric activity. Manufacturing and characterisation of these structures are reported along with the thermal and electrical properties of the graphene-ink employed in this work, enabling low cost pyroelectric energy harvesters capable of converting radiation energy into electrical energy. Furthermore, employing a low cost screen printing process that uses a biocompatible[15] graphene-ink, enables electrode deposition on large pyroelectric substrates[16], printed electronics[17], capacitors[18] and transistors. This extends the range of potential applications to the biomedical, energy, power and signal processing fields.

2. Pyroelectric laminate structures

Due to the intrinsic electro-active properties of pyroelectric materials, direct thermal to electrical energy conversion enables small-scale energy harvesting devices to operate at low temperatures below 80 °C. For an externally induced change in temperature dT (K), the change in spontaneous polarisation dPs_{ij} (C/m^2) in a pyroelectric material is defined by the pyroelectric coefficient p^* (C/m^{2}K), which indicates the thermal to electrical conversion activity of the material[19]:

$$dPs_{ij} / dT = dPs_{ij} / dT \,.\, dT = p^*.dT \qquad (1)$$

Pyroelectrics are a subgroup of piezoelectric materials which experience a change in Ps_{ij} when exposed to mechanical stress (σ) and strain (ε). Therefore, the change in spontaneous polarisation can be a combination of its primary pyroelectric coefficient p^* and secondary contribution ($d_{ij}.c_{ijk}.\alpha_i$) due to a thermal strain and piezoelectric contribution, where the change in polarisation dPs_{ij} with respect to the change in temperature dT is as follows[19]:

$$dPs_{ij} / dT = (p^*+d_{ij}.c_{ijk}.\alpha_i)dT \qquad (2)$$

This can be rearranged to give[11]:

$$dPs_{ij} / dT = p^* - d_{ij}.c_{ijk}\,(\alpha_i - dS_{ij}/dT) \qquad (3)$$

for a symmetrical electrode-pyroelectric-electrode laminate configuration with a piezoelectric coefficient d_{ij}, a mechanical stiffness $c_{ijk,}$, a material thermal expansion α_i, and a thermally induced strain dS_{ij}/dT. According to **equation 3**, a pyroelectric material with a high pyroelectric coefficient p^* as well as a high piezoelectric coefficient d_{ij} is desirable for large changes in dPs_{ij}, leading to an effective electrical signal in response to the induced change in temperature dT. Since the pyroelectric and piezoelectric coefficients indicate the energy conversion performance of a material, the required change in temperature is determined by the thermal design of the energy harvesting device. For the case of thermal radiation heating, the exposed pyroelectric device follows Kichhoff's Law of

electromagnetic wave absorption, reflectance and transmittance. Consequently, the induced change in temperature dT (**equation 3**) derived from the available thermal source power (T_{Source}) perpendicular to the black body surface temperature (T_{Device}), needs to satisfy the Stefan-Bolzmann's law:

$$F = \alpha.A\ (T^4_{Source} - T^4_{Device}) = \alpha.A.dT^4 \quad (4)$$

which determines the available radiant flux F (W/m^2) governed by the surface area A (m^2), the Stefan-Bolzmann constant $\sigma_B = 5.671\text{x}10^{-8}$ (W m^{-2} K^{-4}) and the heat source temperature T_{Source}. Assuming a constant radiation heat source condition, the effective change in temperature is then maximised for a black body surface electrode with a radiation absorption coefficient $\alpha = 1$, which fully utilises the available radiation energy. With respect to the transient change in temperature dT and the pyroelectric coefficient p^*, the effective temperature induced change in polarisation can be directly measured as the pyroelectric short circuit current[20]:

$$I = p^* A.dT/dt \quad (5)$$

and the open circuit voltage:

$$V = p^*/\varepsilon_o\, t.dT \quad (6)$$

with the surface area A (m^2) and the geometrical thickness t (m) across the polarisation direction. Assuming a parallel plate capacitor geometry for the pyroelectric device structure, the available potential difference and the electrical energy E stored in the capacitive pyroelectric element ($E = ½\ C.V^2$) translates to[20]:

$$E = ½\ p^2/\varepsilon.\ A.t.(\Delta T)^2 \quad (7)$$

for the given geometrical dimensions, effective permittivity ε (F/m) and the temperature change experienced by the material, ΔT. In order to optimise the sandwiched pyroelectric electrode architecture towards a greater change in polarisation dPs, the electro-active components p^* and d_{ij} (**equation 3**) of the pyroelectric materials and the radiation absorption α (**equation 4**) of the electrode material need to be maximised to maximise the temperature change.

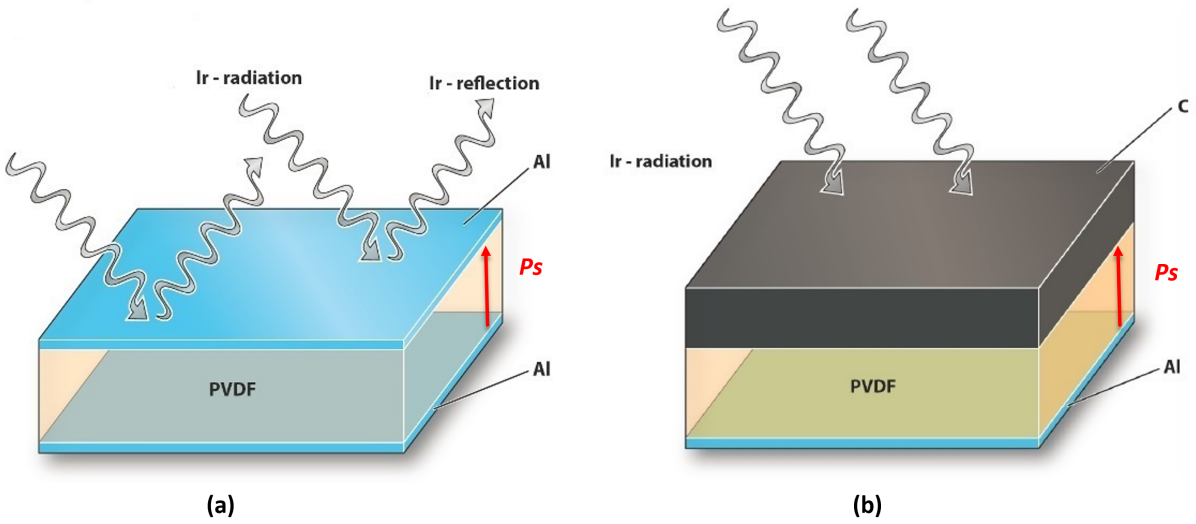

Figure 1: Thermal radiation heating principle for a reflective pyroelectric PVDF/aluminium electrode device (a) and an absorbent asymmetric PVDF/graphene-ink pyroelectric device (b).

Figure 1 compares the principles of radiation heat absorption and reflection (illustrated by wavy arrows) for a reflective aluminium (Al) electrode structure and absorbing black graphene–ink (C) layered electrode structure when exposed to an infra-red (IR) source. The evaporated aluminium electrode employed in **Figure 1a** absorbs 0.22 of the available thermal radiation energy and reflects most of the available heat[21]. For the graphene-ink electrode structure in **Figure 1b**, it is approximated that within the relevant wavelength spectrum of 400 to 900 nm the graphene nanoplatelets (GNPs) dispersed in the terpolymer of vinyl chloride, vinyl acetate and vinyl alcohol-ink binder act as a 'black body' absorber with a constant absorbance[22] of 0.97. The GNPs with a typical thickness of < 50 nm and a platelet size of 0.3 – 5 µm were synthesised in a graphite reduction process and dispersed in the adhesive binder to form a dispensable electrically conductive ink[15] with a bulk density of 215 kg m^{-3}.

When using free standing PVDF films for pyroelectric energy harvesting, the narrow temperature window of the pyroelectric active β-phase between -40 ºC and 120 ºC requires low temperature manufacturing techniques, limiting the number of potential electrode materials. For improved device performance, structurally thick metallic electrodes require high manufacturing temperatures when using conventional sputtering or evaporation techniques, for which reason screen printed carbon based graphene-ink electrodes are employed in this study. **Table 1** compares the thermal conductivity (k), which is important to achieve a rapid and large heat transfer, electrical surface resistance (α_r), for the electrical conductivity across the generator terminals, and radiation absorbance of industrially used metallic pyroelectric electrode materials and the graphene-ink employed in this paper..

Table 1: Thermal conductivity, surface resistance and radiation absorbance for selected pyroelectric electrode materials.

Electrode material	**Thermal conductivity k [W/mK]**	**Surface resistance a_r [Ω/sqr]**	**Absorbance α [-]**	**Reference [-]**
Aluminium	237.0	0.6	0.22	21, 23
Gold	318.0	0.1	0.20	26
ITO	10.2	10.0	0.15	24, 25
Graphene-ink	1.8	65.0	0.97	22

According to **Table 1**, metallic electrode materials, such as aluminium and gold, have high thermal and electrical conductive conductivity, but low radiation absorbance. Absorption values in the range of 0.1 - 0.3 reflect most of the available thermal energy at the electrode surface and lead to small change in temperature at the pyroelectric active material. In comparison, the graphene-ink electrode material employed in this work absorbs most of the available radiation heat energy, thereby maximising the rate of change in temperature dT/dt (**equation 4 and 5**) and the absolute change in temperature dT (**equation 6**) and improving pyroelectric energy harvesting device performance and effectiveness. When employing electrodes which are highly absorbant to radiation for pyroelectric energy harvesting, the theoretical limit of the presented approach is defined by an ideal 'black body' absorber with an absorption maximum of $\alpha = 1$. This constrains the possibility of further optimisation in terms of reducing reflection losses.

2.1. Screen printed graphene-ink on pyroelectric PVDF

Graphene ink, HDPlas Sc213, supplied by Haydale Ltd. (Wales-UK), was used as upper electrode material for a pre-poled 52 µm thick β-phase PVDF film (Precision Acoustics – UK) with a relative permittivity $\varepsilon_r = 11$. The polarisation characteristics, indicating the pyroelectric activity of the PVDF film used, are provided in the supplementary information (S1)[4]. As shown in **Figure 2**, the graphene-ink electrode was screen printed using an ATMA AT - 25PA (US) screen printing set-up with a squeegee speed of 220 mm.sec−1 at constant pressure (squeegee material: Shore 70A 0605) on a flat PVDF sheet.

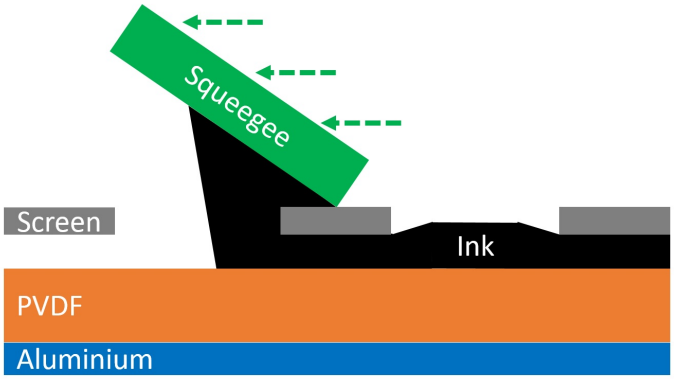

Figure 2: Schematic of the graphene–ink screen printing deposition process on PVDF showing the 'squeegee' spreading the ink across the screen mask.

The extrusion manufactured PVDF film was held in place by a screen printing mask. Following an extensive drying period of one day at room temperature, subsequent thickness measurements across the edges, the corners and the centre were conducted using a Dektak (US) surface profiler. With an average thickness of 9 µm (± 10 %), the screen printed graphene-ink on flat PVDF has a homogeneous thickness maintaining flexibility with a PVDF to electrode thickness ratio of 5.8 (52/9).

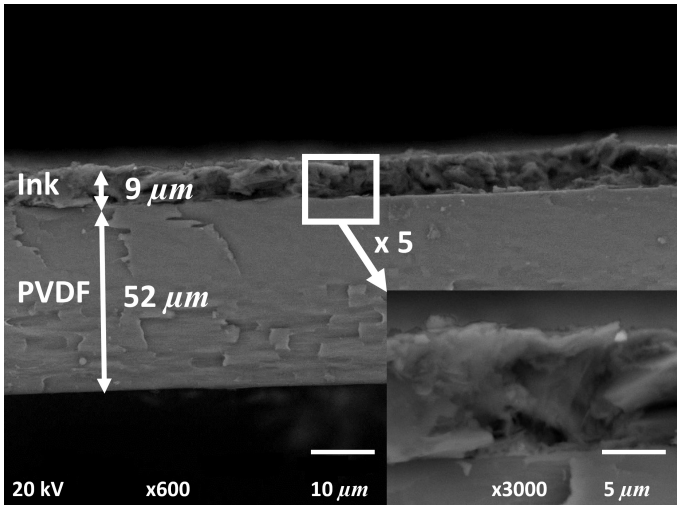

Figure 3: Cross-section SEM image of PVDF/graphene-ink pyroelectric energy harvesting device.

For the thick PVDF/graphene-ink structure from **Figure 1b**, **Figure 3** shows a cross-section view scanning electron micrograph (SEM) image of the pyroelectric device. The GNPs dispersed in the ink binder provide high electrical and thermal bulk conductivity[15]; also see Table 1. For the back electrode, a 200 nm thick electron beam vapour deposited (Edwards FL-400) aluminium was used. The asymmetric PVDF/graphene-ink/aluminium pyroelectric energy harvesting device (**Figure 1b**) is significantly thicker than the standard metallic aluminium reference design (**Figure 1a**), due to the higher thickness of the graphene-ink electrode material and the screen printing deposition technique. With a sample surface area of (2x2) cm^2, the asymmetric graphene-ink/PVDF/aluminium energy harvesting device had a pyroelectric coefficient of -27 $\mu C/m^2K$[19].

2.2. Electrical properties of polymer based graphene-ink

In order to characterise the electrical conductivity of the screen printed graphene ink electrode and the suitability for pyroelectric structures, the electrical surface resistance was measured. With a linearly arranged Jandel (UK) four point probe (tungsten carbide with a probe spacing of 5 mm needle to needle), bipolar line sweep calibration measurements against reference indium tin oxide (ITO) on a glass substrate were conducted. From Ohm's law, the surface resistance for a voltage-current sweep determines the sheet resistance for the test surface. The manufactured screen printed graphene electrodes had a measured surface resistance of α_r = 65 Ωsqr^{-1} (± 10 %) as compared to a highly conductive metallic aluminium electrode with a surface resistance[23] of α_r = 2 Ωsqr^{-1}, the thick layered graphene-ink electrode is over 30 times more resistive, leading to higher parasitic losses across the electrodes.

2.3. Thermal properties of polymer based graphene-ink

Bulk thermal conductivity measurements for the screen printed graphene-ink were conducted according to ISO8301 and ASTM C518 standards using a TA Instruments (US) Fox 50 measuring

setup. Prior to the measurement, the ink was screen printed (1.2 mm thick) on a copper disc (50 mm diameter and 0.45 mm thick). In order to prevent surface thermal resistance, the sample was placed between two Peltier elements and the surface contact was ensured a using copper grease. Since the thin copper disc has a high thermal conductivity compared to the relatively thick graphene-ink sample, thermal conduction dominates between the two Peltier devices, deriving the thermal resistance parameter of the printed graphene-ink from a Lumped capacity model. With an average thermal conductivity value k of 1.8 $Wm^{-1}K^{-1}$ at 20, 40 and 60 °C, the insulating nature of the ink is lower than the reported values ranging from 8.7 $Wm^{-1}K^{-1}$ for graphite to 2900 $Wm^{-1}K^{-1}$ for individual 2D graphene sheets[22]; this is likely to be due to the binders used in the ink and the GNPs used, rather than 2D sheets.

2.4. Harmonic temperature oscillations for pyroelectric energy harvesting

In order to test the pyroelectric device under constant thermal boundary conditions, external temperature oscillations were performed by switching an IR lamp (Phillips PAR38 175 Watt) at 340 mW/cm^2 (measured using a calibrated thermal power sensor - THORlabs Germany with a peak wavelength at 700 nm) periodically 'ON' and 'OFF' using a variable frequency controller. When the light was switch 'ON', the pyroelectric test device was exposed perpendicularly to the radiation beam and when the light was switched 'OFF', free convection cooled the pyroelectric. Free air convection cooled the sample on each side, assuming a constant room air temperature of 22 °C. Since the test samples were exposed from one side (top down) to the IR radiation beam at a distance of 15 cm, uniaxial radiative heating similar to solar radiation was performed. Temperatures were captured once a thermal equilibrium was established and the average temperature of the specimen remained constant. The temperature was constant when the lamp ’ON’ time was equal to the ’OFF’ time duration. The change in temperature was measured at the electrode surface using leaf-type thermocouples (OMEGA -US) along with the open circuit voltage and closed circuit current using a Keithley (US) 6517 high input impedance electrometer (200 TΩ). The complete test system in shown in Fig. S2.

3. Experimental results

The intrinsically different photo-thermal heating and the convective cooling effects, when using an IR radiation test set-up, leads to a complex temperature profile across the pyroelectric energy harvesting device. **Figure 4** compares the surface electrode temperature at the top (upper temperature envelope) and at the bottom electrode (lower temperature envelope) for the uni-axial heated pyroelectric devices over 60 sec for both the graphene-ink and aluminium electrodes. At a lamp switching frequency of 0.05 Hz, the surface temperature for the graphene-ink electrode and the reference aluminium electrode was measured over three thermal cycles at constant average temperatures, indicated by the ‘ON’ and ‘OFF’ regions in **Figure 4**. Compared to the aluminium reference electrode, the graphene-ink electrode average temperature, absolute temperature (T) and the rate of change in temperature (dT/dt) was significantly different. Considering the first 10 sec. of the heating wave in

Figure 4, the surface temperature increase from 28 to 33 ºC for the graphene-ink electrode is 5 K, compared to the smaller temperature increase of 2 K between 29 and 31 ºC for the aluminium reference electrode, leading to more thermal radiation energy being absorbed by the graphene-ink pyroelectric device.

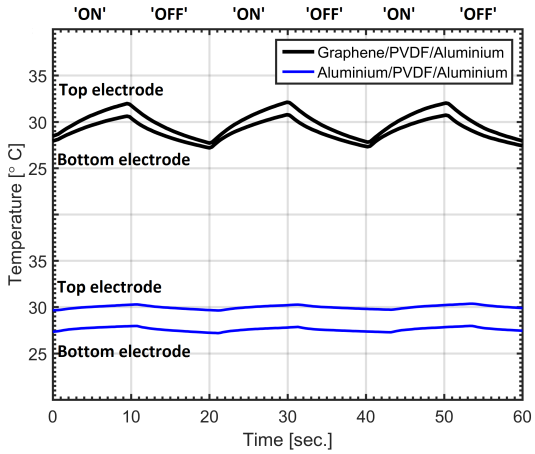

Figure 4: Temperature profile for the top and bottom electrode for the conventional PVDF/aluminium electrode (blue) device and asymmetric PVDF/graphene-ink pyroelectric energy harvesting device (black).

In addition to the higher temperature level achieved with graphene-ink structures, the difference between top and bottom electrode temperature in **Figure 4** shows an increase from 0.5 K (at 0 sec.) to 3 K (at 10 sec.) over the first 10 sec. of heating. Compared to the constant top and bottom temperature difference of 2 ºC for the aluminium/PVDF/aluminium laminate, the time variant temperature gradient over time with the graphene-ink/PVDF/aluminium sample is due to a complex thermal conductivity between the top and bottom electrode across the sample thickness. When using an unclamped sample fixture, a buckling behaviour of the square shaped graphene-ink/PVDF/aluminium film was observed. Since all pyroelectric systems are also piezoelectric, the relatively thick 2-2 connectivity graphene-ink/PVDF/aluminium sample consequently experienced piezoelectric activity due to the interface coupling between surfaces, inducing tangential shear stress when thermally excited[12]. **Figure 5** presents the pyroelectric device activity in response to the corresponding performed changes in temperature, as shown in **Figure 4**. The corresponding rate of change in temperature (*dT/dt*) for the graphene-ink and the aluminium design in **Figure 5a** uses the time forward derivative. For the graphene-ink device, the rate of change in temperature is 7.5 times higher (1.5 K/s) for the heating and cooling cycle compared to the aluminium reference electrode (0.2 K/s).

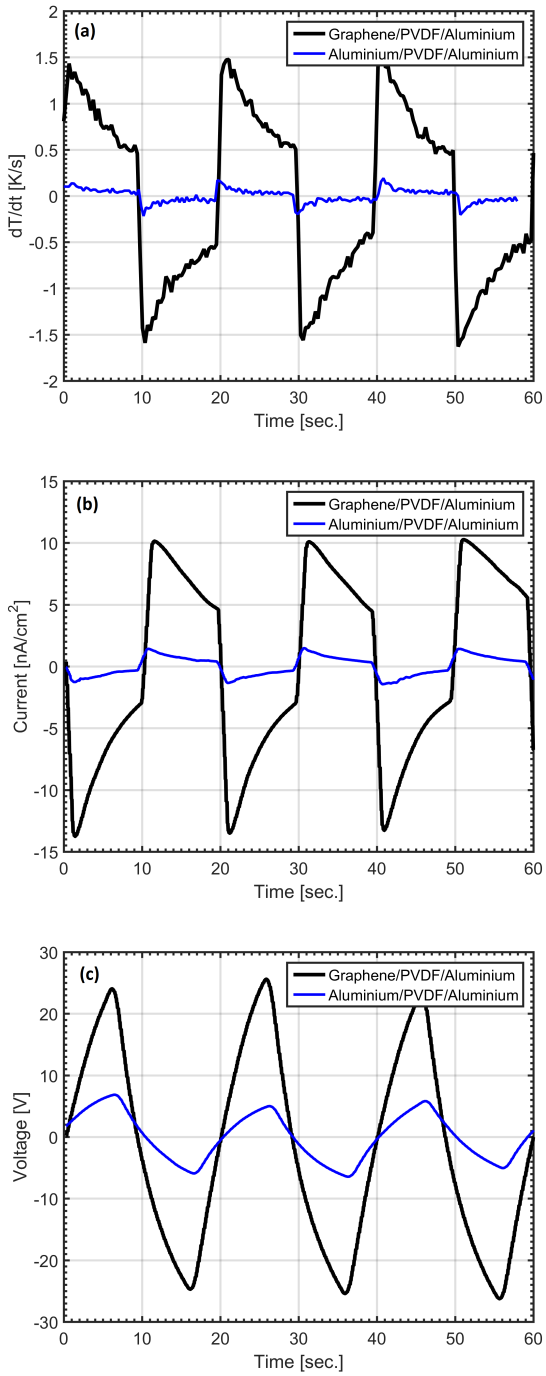

Figure 5: Rate of change in temperature dT/dt (a), closed-circuit current (b) and open-circuit voltage (c) for Aluminium electrode and PVDF/graphene-ink pyroelectric energy harvesting device.

According to equation 5, the closed circuit pyroelectric current is then proportional to the rate of change in temperature (dT/dt), determining the direct energy conversion effectiveness with a peak at the transition of each thermal cycle. Figure 5b compares the measured closed circuit current with respect to the performed changes in temperature for the graphene-ink and aluminium device (Figure 4). Due to the different heat transfer principles for heating (radiation) and cooling (free convection), the graphene-ink samples shows a peak current of 14 nA cm^{-2} for radiation heating and a peak current

of 10 nA cm^{-2} for convective cooling. Comparing the symmetric 2 nA cm^{-2} current of the aluminium/PVDF/aluminium electrode with the graphene/PVDF/aluminium, the graphene-ink based sample performs 7 times better with radiation heating and 5 times better for convective cooling than the aluminium reference electrode. According to the 7.5 times higher rate of change in temperature (*dT/dt*) for the graphene ink device in Figure 5a, the measured closed circuit current is 7 times better with graphene-ink/PVDF/aluminium. This leads to the conclusion, that the improved device performance exclusively attributed to the thermal effect of high radiation absorbance (primary pyroelectric effect), neglecting the secondary contribution. Since the average temperatures are constant over time, the symmetric open circuit voltage of the graphene-ink electrode system with a peak of 24 V at the end of each thermal cycle, see **Figure 5c,** is 3.4 times higher than the open circuit voltage of 7 V with the aluminium electrode, confirming the closed circuit current measurements. Since the energy stored in the electric potential difference is time variant, pyroelectric generators require rectification in order to supply external electronics with a direct current (DC). In this work, a full wave bridge rectifier was formed from four diodes (Vishay GP02) and the harvested radiation energy was stored in an external 100 nF capacitor (AVX), and measured as voltage at the capacitor terminals[27].

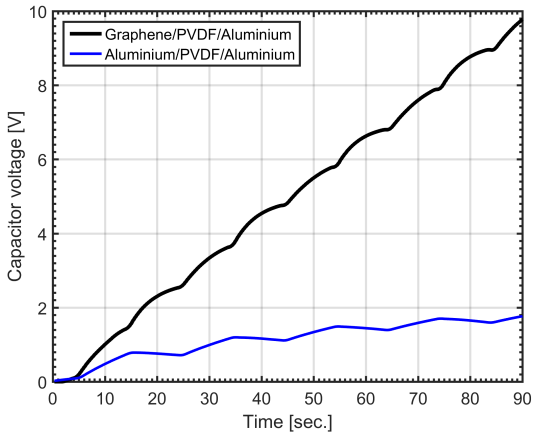

Figure 6: Harvested energy with PVDF/graphene-ink pyroelectric energy harvesting device and stored in an external capacitor.

Figure 6 compares the harvested energy using the graphene-ink/PVDF/aluminium and the aluminium/PVDF/aluminium devices over several thermal cycles, when rectified and discharged through the rectification circuit into an external storage capacitor. After 90 sec. of harvesting thermal radiation from the lamp, the graphene-ink based sample charged the external storage capacitor to 10 V compared to the 1.9 V for the aluminium, outperforming aluminium electrode device by over 5 times and over 25 times (**equation 7**) for the harvested energy due to the squared relationship for the capacitor voltage.

The experimental set-up compares reproducible experimental thermal radiation measurements

for screen printed graphene-ink electrodes and standard metallic aluminium electrodes on PVDF. Assuming a parallel plate geometry for the device architecture employed here, the pyroelectric harvesters have an electrical capacitance of 750 pF (relative permittivity[28] for the PVDF film ε_r= 11) followed by a peak energy density of 1.13 μJ/cm^3 at 24 V. Further improvements in energy density and generator effectiveness are expected when using lead zirconate titanate (PZT)[18] crystalline ceramics or lead magnesium niobate-lead titanate (PMN-PT) single crystals[29] as pyroelectric active material with a higher pyroelectric coefficient of 380 μC/m^{2}K and 1790 μC/m^{2}K, respectively (**equation 3, 5** and **6**); although large scale deformation due to thermal mismatch is unlikely in there much stiffer materials. A mechanical model could be of interest to develop for the buckling behaviour of the graphene/PVDF/aluminium structure when heated or cooled, and take into account the thermal expansion and the mechanical properties of the graphene-ink in order to assess the pyroelectric secondary contribution for the energy harvesting system along with a detailed analysis of the adhesion between the laminates.

4. Conclusions

This paper has examined the significant improvements achieved in the pyroelectric performance of novel graphene/PVDF/aluminium laminate systems under thermal oscillations. Under constant thermal radiation heat source conditions, the high absorbance graphene-ink electrodes perform 3.4 times better under open and closed-circuit conditions and over 25 times better when rectified in pyroelectric generator mode, compared to conventional aluminium electrodes. The proposed design is viable on a device level due to ease of screen-printing and enabling low cost pyroelectric energy harvesting devices on a large scale. The novel asymmetric graphene/PVDF/aluminium structure was experimentally proven along with a complete discussion of the device manufacturing and graphene-ink characterisation in terms of electrical and thermal properties. The dispersed GNPs in the ink show a sufficiently high thermal conductivity of 1.8 W/mK and a surface electrical conductivity of 65 Ωsqr^{-1} for harvesting applications, although additional improvements in electrical and thermal conductivity would further improve the harvesting potential. The significant benefits of the graphene-ink electrode were also observed by rectification and storage of generated charge in an external capacitor. With the asymmetric laminate structure, the flexible pyroelectric energy harvesting device operates as a small scale generator, fully utilising the available radiation energy due to the high thermal absorbance. In addition, the here employed flexible graphene-ink can be used as electrode material for printed electronic circuits or black-body coating for sensor and heat dissipation applications.

5. Acknowledgements

The research leading to these results has received funding from the European Research Council under the European Union's Seventh Framework Programme (FP/2007-2013)/ERC Grant Agreement No. 320963 on Novel Energy Materials, Engineering Science and Integrated Systems. The graphene-

ink and the ATMA screen printing facilities used in this work were supplied by Haydale Ltd (UK). Thermal conductivity measurements for the graphene-ink were conducted by John Gearing Scientific Ltd. (UK).

6. References

[1] Bowen, C.R., Kim, H.A., Weaver, P.M. and Dunn, S., 2014. Piezoelectric and ferroelectric materials and structures for energy harvesting applications. *Energy Environ. Sci., 7*(1), pp.25-44.

[2] Sebald, G., Guyomar, D. and Agbossou, A., 2009. On thermoelectric and pyroelectric energy harvesting. *Smart Mater. Struct., 18*(12), pp.125006.

[3] Hanrahan, B., Neville, C., Smith, A., Ter-Gabrielyan, N., Jankowski, N. and Waits, C.M., 2016. Wireless Power Transmission via Modulated Laser Irradiation of Pyroelectric Thin Films. *Adv. Mater. Technol.*, *1*(9), pp.1-5.

[4] Zabek, D., Taylor, J., Boulbar, E.L. and Bowen, C.R., 2015. Micropatterning of Flexible and Free Standing Polyvinylidene Difluoride (PVDF) Films for Enhanced Pyroelectric Energy Transformation. *Adv. Energy Mater.*, *5*(8), pp.1-6.

[5] Cuadras, A., Gasulla, M. and Ferrari, V., 2010. Thermal energy harvesting through pyroelectricity. *Sens. Actuators, A*, *158*(1), pp.132-139.

[6] Wang, S., Wang, Z.L. and Yang, Y., 2016. A One-Structure-Based Hybridized Nanogenerator for Scavenging Mechanical and Thermal Energies by Triboelectric–Piezoelectric–Pyroelectric Effects. *Adv. Mater.*, *28*(15), pp.2881-2887.

[7] Lin, L., Hu, Y., Xu, C., Zhang, Y., Zhang, R., Wen, X., and Wang, Z. L., 2013. Transparent flexible nanogenerator as self-powered sensor for transportation monitoring. *Nano Energy*, *2*(1), pp.75-81.

[8] Zhao, T., Jiang, W., Liu, H., Niu, D., Li, X., Liu, W., Li, X., Chen, B., Shi, Y., Yin, L. and Lu, B., 2016. An infrared-driven flexible pyroelectric generator for non-contact energy harvester. *Nanoscale*, *8*(15), pp.8111-8117.

[9] Battista, L., Mecozzi, L., Coppola, S., Vespini, V., Grilli, S., and Ferraro, P., 2014. Graphene and carbon black nano-composite polymer absorbers for a pyro-electric solar energy harvesting device based on $LiNbO_3$ crystals. *Appl. Energy*, *136*, pp.357-362.

[10] Moalla, R., Vilquin, B., Saint-Girons, G., Sebald, G., Baboux, N. and Bachelet, R., 2016. Dramatic effect of thermal expansion mismatch on the structural, dielectric, ferroelectric and pyroelectric properties of low-cost epitaxial PZT films on SrTiO 3 and Si. *CrystEngComm*, *18*(11), pp.1887-1891.

[11] Newnham, R.E., Skinner, D.P. and Cross, L.E., 1978. Connectivity and piezoelectric-pyroelectric composites. *Mater. Res. Bull., 13*(5), pp.525-536.

[12] Chang, H.H.S. and Huang, Z., 2008. Substantial pyroelectric effect enhancement in laminated composites. *Appl. Phys. Lett.*, *92*(15), p.152903.

[13] Chang, H.H.S. and Huang, Z., 2009. Pyroelectric effect enhancement through product property under open circuit condition. *J. Appl. Phys.*, *106*(1), p.014101.

[14] Kesim, M.T., Zhang, J., Alpay, S.P. and Martin, L.W., 2014. Enhanced electrocaloric and pyroelectric response from ferroelectric multilayers. *Appl. Phys. Lett.*, *105*(5), p.052901.

[15] www.hadayle.com (Accessed: 04.12.2016).

[16] El Fatnani, F. Z., Guyomar, D., Mazroui, M. H., Belhora, F., and Boughaleb, Y., 2016. Optimization and improvement of thermal energy harvesting by using pyroelectric materials. *Opt. Mater.*, *56*, pp.22-26.

[17] Grande, L., Chundi, V. T., Wei, D., Bower, C., Andrew, P., and Ryhänen, T., 2012. Graphene for energy harvesting/storage devices and printed electronics. *Particuology*, 10(1), pp.1-8.

[18] Yu, G., Xie, X., Pan, L., Bao, Z., and Cui, Y., 2013. Hybrid nanostructured materials for high-performance electrochemical capacitors. *Nano Energy*, 2(2), pp.213-234

[19] Lang, S.B. and Das-Gupta, D.K., 2000. Pyroelectricity: fundamentals and applications. *Handbook of advanced electronic and photonic materials and devices*, *4*, pp.22-50.

[20] Bowen, C.R., Taylor, J., LeBoulbar, E., Zabek, D., Chauhan, A. and Vaish, R., 2014. Pyroelectric materials and devices for energy harvesting applications. *Energy Environ. Sci., 7*(12), pp.3836-3856.

[21] Bartl, J. and Baranek, M., 2004. Emissivity of aluminium and its importance for radiometric measurement. *Meas. Sci. Rev.*, *4*(3), pp.31-36.

[22] Yu, A., Roes, I., Davies, A. and Chen, Z., 2010. Ultrathin, transparent, and flexible graphene films for supercapacitor application. *Appl. Phys. Lett.*, *96*(25), p.253105.

[23] Pears, C.D. in Touloukian, Y.S., Powell, R.W., Ho, C.Y. and Klemens, P.G., 1971 Thermophysical and Electronic Properties Information and Analysis, *TPRC Data Series, 2*, p.145-6.

[24] Thuau, D., Koymen, I. and Cheung, R., 2011. A microstructure for thermal conductivity measurement of conductive thin films. *Microelectron. Eng.*, *88*(8), pp.2408-2412.

[25] Kim, H., Gilmore, C.M., Pique, A., Horwitz, J.S., Mattoussi, H., Murata, H., Kafafi, Z.H. and Chrisey, D.B., 1999. Electrical, optical, and structural properties of indium–tin–oxide thin films for organic light-emitting devices. *J. Appl. Phys.*, *86*(11), pp.6451-6461.

[26] www.goodfellow.com/E/Gold.html (Accessed: 04.12.2016).

[27] Zabek, D., Taylor, J. and Bowen, C.R., 2016. Characterization and Modeling of Meshed Electrodes on Free Standing Polyvilylidene Difluoride (PVDF) Films for Enhanced Pyroelectric Energy Harvesting. *IEEE Trans. Sonics Ultrason.*, *63*(10), p.1681.

[28] Precision-Acoustics-Ltd., Dorset, 2013. *PVDF Properties and Uses*, Available: http://acoustics.co.uk/wp-content/uploads/2013/12/Properties-ofpoled-PVDF.pdf (Accessed: 04.12.2016)

[29] Wu, F., Cai, W., Yeh, Y.W., Xu, S. and Yao, N., 2016. Energy scavenging based on a single-crystal PMN-PT nanobelt. *Sci. Rep.*, *6*, pp.1-10.

Supplementary information to:

Graphene-Ink Laminate Structures on Polyvinylidene Difluoride (PVDF) for Pyroelectric Thermal Energy Harvesting and Waste Heat Recovery

Daniel Zabek* [a], Kris Seunarine[b], Chris Spacie[b], and Chris Bowen[a]

[a]University of Bath, Claverton Down, BA2 7AY, Bath, UK.

[b]Haydale Ltd., Ammanford, SA18 3BL, UK.

*email: D.Zabek@bath.ac.uk

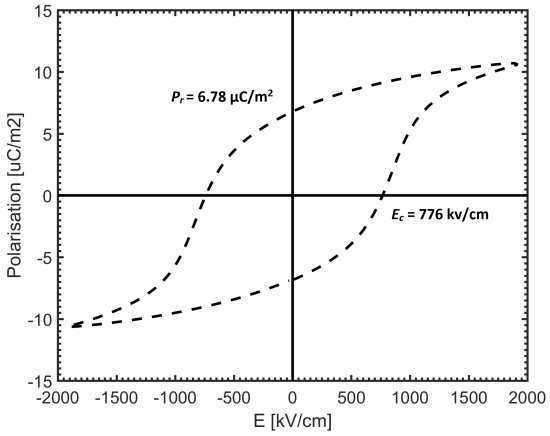

S1: Polarisation (P) - applied electric field (E) for the employed PVDF film [4].

The extruded 52 µm thick corona poled PVDF film has a remnant polarisation P_r of 6.78 µC/cm^2 and a coercive field E_c of 776 kV/cm from the tested P-E loop.

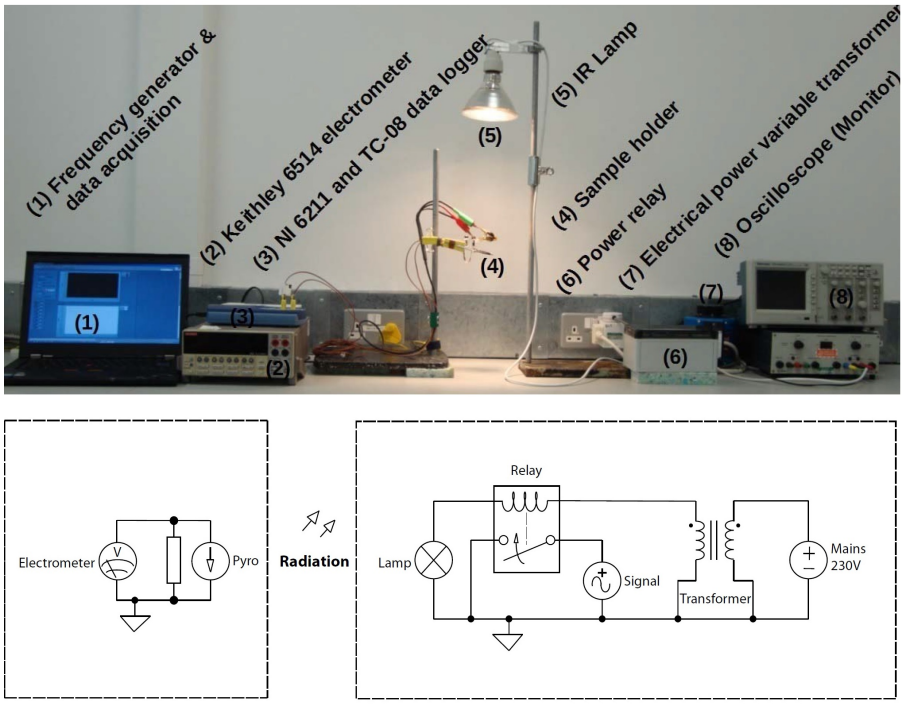

S2: Radiation pyroelectric setup for thermal energy harvesting.

Fig S2. Shown the experimental setup.

TOC graphic: